

# Estimating the initial temperature of the Quark-Gluon Plasma with Quarkonia

—  
ELTE haladó labor 2017/I. *HEP-HF*

Róbert Vértesi

April 26, 2017

## Abstract

This booklet is an extension to Ref. [1] (in Hungarian). In the measurement described here we estimate the temperature of the strongly interacting Quark-Gluon Plasma (sQGP) by observing the sequential melting of quarkonium (two  $\Upsilon$  states in particular) in pseudo-RHIC Au+Au collision data at  $\sqrt{s_{NN}} = 200$  GeV.

## Contents

<b>1</b>	<b>Introduction</b>	<b>1</b>
<b>2</b>	<b>Steps of the measurement</b>	<b>2</b>
2.1	Dataset and observation . . . . .	2
2.2	Decay kinematics and detection . . . . .	3
2.3	Invariant mass peak and the yield . . . . .	4
2.4	Determining the nuclear modification . . . . .	5
2.5	Inferring the initial temperature . . . . .	5
<b>3</b>	<b>Summary of the tasks</b>	<b>5</b>

## 1 Introduction

In ultrarelativistic heavy ion collisions, a phase transition occurs from hadronic matter into a state of deconfined quarks and gluons [1, 2, 3]. This latter state of matter, dubbed as the strongly interacting Quark Gluon Plasma (sQGP), has been a subject of extensive measurements at the Relativistic Heavy Ion Collider (RHIC), and more recently at the Large Hadron Collider (LHC). Significantly higher luminosity of these colliders in the recent years, paired with continuous detector development allows one to turn to rare probes, such as heavy flavor (charm and bottom quark) production, which are complementary to observables of light hadrons and provide us with a deeper understanding of the strong interaction.

Charm and bottom quarks are produced in hard QCD processes early in the interaction, and, due to their large masses, their number is virtually unaffected in the later stages of the reaction. On the other hand, their lifetimes are high enough to survive up to the point where the dense medium is no longer present. Heavy flavor quarks therefore provide a unique means of exploring the properties of the sQGP.

A heavy quark-antiquark pair can form a bound state, the so called quarkonium. Bound  $c\bar{c}$  and  $b\bar{b}$  states are called charmonia and bottomonia, respectively. It has long been suggested that, due to the screening of the heavy quark potential, the production of quarkonia is suppressed in heavy ion collisions compared to expectations from p+p collisions. Charmonium suppression was, in fact, anticipated as a key signature of quark-gluon plasma (QGP) formation [4]. Moreover, different quarkonium states are expected to dissociate (“melt”) in the QGP at different temperatures due to their different binding

energies. It has therefore been suggested that comprehensive quarkonium measurements can be used as a QGP thermometer [5].

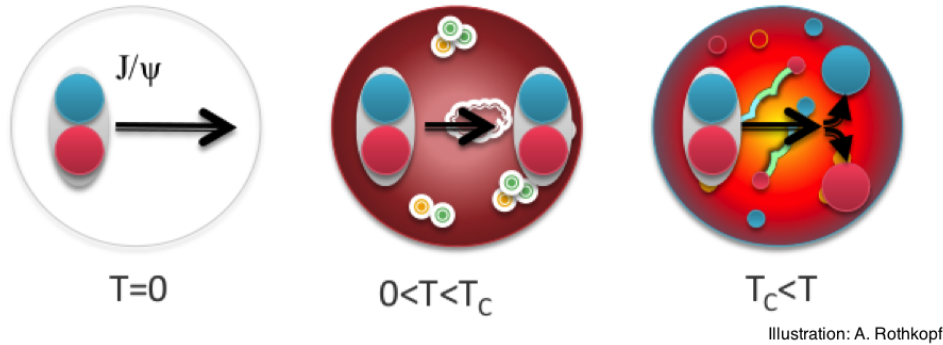


Figure 1: Cartoon showing quarkonium (from left to right) at vacuum temperature, remaining intact in a "cold" hadronic environment below the critical temperature of deconfinement ( $T_c$ ), and dissociating in "hot" deconfined matter above  $T_c$ .

The dissociation of quarkonia in the medium is illustrated in Fig. 1. Production of charmonia (especially the  $J/\psi$  meson) is abundant and therefore it is relatively easy to measure them with precision. However, random recombination of  $c$  and  $\bar{c}$  in the hot plasma, as well as "cold" effects like interactions in the initial state, co-mover absorption in the hadronic phase, or decays of excited states to  $J/\psi$ , influence measured yields [6]. Bottomonium measurements (typically the  $\Upsilon$  mesons) are a cleaner probe because, contrary to charm quarks, the effect of bottom pair recombination and co-mover absorption is negligible at RHIC energies [7].

Recent quarkonium measurements in heavy ion collisions at the LHC and RHIC support the sequential melting hypothesis [8, 9]. Further details on quarkonium production at RHIC energies is in Ref [10].

## 2 Steps of the measurement

The goal is to determine the temperature of the sQGP created at RHIC energies in central Au+Au collisions. To complete that, we will determine the nuclear modification of two Bottomonium states. To infer the temperature, we will compare the results to a model prediction based on the idea of sequential quarkonium melting [13].

### 2.1 Dataset and observation

The work will be done on Monte-Carlo generated pseudo-data samples, produced by the PYTHIA event generator. These samples are ready for our measurement. Proton-proton ( $p+p$ ) collisions were generated with  $\sqrt{s_{NN}} = 200$  GeV center-of-mass energy per nucleon pair, corresponding to RHIC energies. The central nucleus-nucleus (Au+Au) collision samples were mimicked by modifying the  $p+p$  output to include collectivity and plasma effects (radial flow and quarkonium melting). Two of the bottomonium states,  $\Upsilon(1S)$  ( $m_{\Upsilon(1S)} = 9.46$  GeV) and  $\Upsilon(2S)$  ( $m_{\Upsilon(2S)} = 10.02$  GeV) are in the data samples, along with a background from hard QCD processes. Other quarkonium states are not included, for the sake of simplicity.

We observe the  $\Upsilon$  mesons via their  $\Upsilon \rightarrow e^-e^+$  decay channel, corresponding to a branching ratio  $B_{ee} \approx 2.4$  %. Therefore only electrons<sup>1</sup> and electron pairs are stored in the output.

Because of the large  $\Upsilon$  mass, it will be flying rather slowly, but once it decays, the daughter electrons will fly with a high momentum, typically back-to-back. An example of an  $\Upsilon$  decay is shown in Fig. 2.

In a real experiment, the track of the electron is recorded by silicon and gas detectors submerged in a magnetic field. The momentum ( $p$ ) of the electrons is calculated based on their track radius in the magnetic field. Their energy ( $E$ ) is measured in the electromagnetic calorimeter outside the tracking

<sup>1</sup>From here on, the word "electrons" will be collectively used for electrons and positrons.

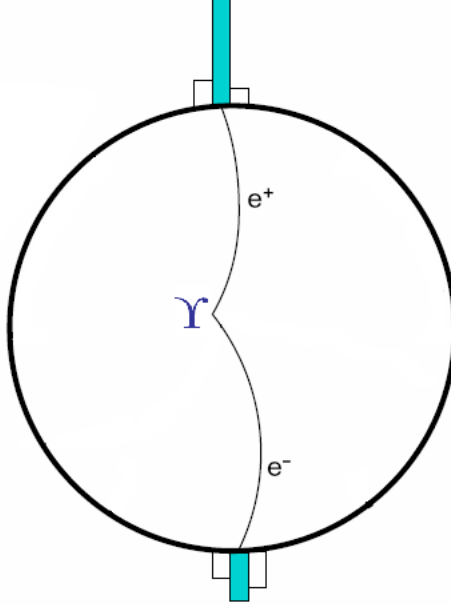


Figure 2: Schematic drawing of an  $\Upsilon$  decay and detection in the  $(x, y)$  plane perpendicular to the beam direction  $z$ . The bars at the ends of the tracks represent the energy deposits in the electromagnetic calorimeter.

system. Since none of the measurements is perfect, the momentum and the energy can be determined by some finite resolution. Typical resolutions are  $\Delta p = 3\%$  and  $\Delta E = (8\sqrt{E/\text{GeV}} + 2)\%$ . The finite resolution effect is taken into account in our simulations.

*Note:* In high energy physics we often use the following kinematical variables:

- Transverse momentum:  $p_{\text{T}}^2 = p_x^2 + p_y^2$  expresses the momentum perpendicular to the beam axis  $z$ .
- Pseudorapidity  $\eta = -\ln(\tan\theta)$ , where  $\theta$  is the angle with respect to the beam axis  $z$ . ( $\eta = 0$  is flying away from the axis in a right angle, and a large  $\eta$  means a small angle to the axis). In case of massless particles, the pseudorapidity equals the relativistic rapidity in longitudinal ( $z$ ) direction.
- azimuthal angle  $\phi$ , the inclination in the  $(x, y)$  plane perpendicular to the beam axis.

## 2.2 Decay kinematics and detection

As a consequence of their large mass, very few heavy-quark containing particles are created in a collision compared to light(er) hadrons species. Therefore we will have a small signal (in our case  $\Upsilon$  mesons decaying to an  $e^-e^+$  pair) in a large background of electrons and positrons from other processes. If we would like to find our signal, it is essential that we define kinematical conditions that will be fulfilled by many of the signals and preferably much less from the background. The conditions should be optimized so that  $\Upsilon$  mesons are selected with a high-enough efficiency  $\epsilon = \frac{N_{\text{selected signal}}}{N_{\text{total signal in the sample}}}$ , keeping the purity  $f = \frac{N_{\text{selected signal}}}{N_{\text{selected signal} + \text{background}}}$  high at the same time. Since the  $\Upsilon$  mesons are massive, at least one of the decay electrons will be very energetic. Based on that, usually a recording-time preselection is already carried out by storing "triggered" data that contains at least one energetic hit in one of the detectors. The signal in our samples has already been enhanced by imposing conditions similar to a strong trigger, so that the signal can easily be seen.

Still, further selection has to be applied to improve sample purity and allow for a reasonable determination of  $\Upsilon$  production. One of the tasks in this measurement is to establish such selection criteria. In the followings, some tips are provided. These are just to give an idea about what to look at. You are encouraged to look at the individual distributions to determine the optimal selection cuts.

- Since  $\Upsilon$  mesons are neutral, they decay into an  $e^-e^+$  pair. Identically charged pairs are only background, no signal.
- The mass of  $\Upsilon$  mesons is  $m_\Upsilon \approx 10 \text{ GeV}/c^2$ . Since most of the decays are relatively symmetric, it is safe to assume that in most of the cases, both the electrons will have a momentum  $p_i > 2$  to  $3 \text{ GeV}/c$ .
- The back-to-back nature of the decays ensure that the angle between the two tracks at their starting points,  $\Delta\phi = \phi_2 - \phi_1$ , will be large enough.

### 2.3 Invariant mass peak and the yield

The invariant mass of an  $e^-e^+$  pair system is expressed in natural units ( $c = 1$ ) as

$$m^2 = E^2 - \mathbf{p}^2 = (E_1 + E_2)^2 - (\mathbf{p}_1 + \mathbf{p}_2)^2 = m_1 + m_2 + 2(E_1E_2 - \mathbf{p}_1\mathbf{p}_2), \quad (1)$$

where  $E$  and  $\mathbf{p}$  without indices are the energy and 3-momentum of the system, and indices 1,2 denote the individual properties of the two daughter electrons. Considering that the electron masses are very small,<sup>2</sup> the first two terms can be neglected. Since the detector resolution in momentum is always better than the energy resolution, we make use of the fact that  $E_i \approx p_i$  and further rewrite the equation as

$$m^2 = 2p_1p_2(1 - \cos\alpha) = 2p_{T1}p_{T2}(\cosh(\eta_1 - \eta_2) - \cos(\phi_1 - \phi_2)). \quad (2)$$

where  $\alpha$  is the angle between the two tracks.

If an  $e^-e^+$  pair comes from the decay of an  $\Upsilon$ , the reconstructed invariant mass is likely around the rest mass of the parent meson. Looking at the invariant mass distribution, the peaks corresponding to the  $\Upsilon$  states will be visible on top of the background. Because the  $\Upsilon$  mesons are long-lived, their Breit-Wigner peak is very narrow. The measured peaks can therefore be characterized by a Gaussian corresponding to our finite detector resolution. However, one more effect to consider is that some of the electrons lose energy via Bremsstrahlung, thus distorting the mass peak. We therefore describe the  $\Upsilon \rightarrow e^-e^+$  mass peak with a so called Crystal Ball function  $f_{CB}(x)$ , that is actually a Gaussian with a long power-law tail towards lower mass values [14]. It is described with 5 parameters altogether including overall normalization, see Fig. 3.

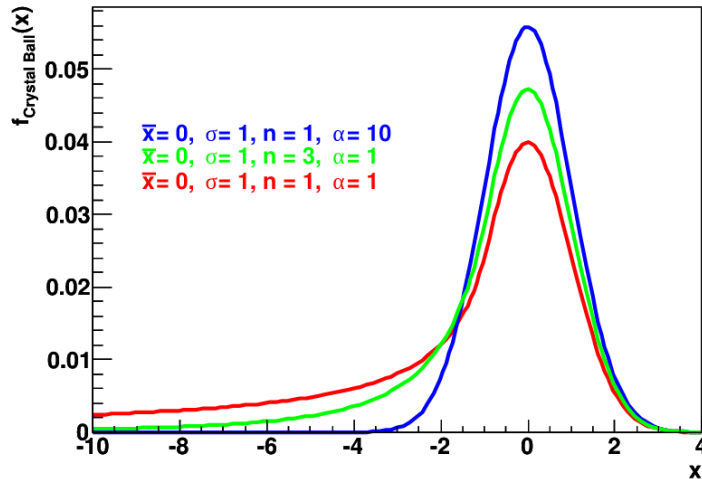


Figure 3: Examples of the Crystal Ball function. (Source: Wikimedia commons.)

There are also  $e^-e^+$  pairs that do not come from  $\Upsilon$  decays, just happen to be in the same mass range. In order to determine the yield we have to understand how many of the hits under the invariant mass peak come from the background. We approximate the background with a reciprocal power law function  $f_{BG}(x) = \frac{N}{(1+x/a)^b}$ . This function shape is known to model well the distributions of correlated

<sup>2</sup>The electron mass is 511 eV, which compares to our energy scale of several GeVs.

electrons from concurrent processes [9]. To figure out how large our peaks are, we fit a compound function  $f(m) = f_{\text{BG}}(m) + f_{\text{CB}}^{\Upsilon(1\text{S})}(m) + f_{\text{CB}}^{\Upsilon(2\text{S})}(m)$  on the invariant mass distribution. Since this function has altogether  $3+5+5=13$  parameters, it would be very difficult to achieve convergence if all are varied. Therefore we first fit  $f_{\text{CB}}^{\Upsilon(1\text{S})}(m)$  and  $f_{\text{CB}}^{\Upsilon(2\text{S})}(m)$  on the clean  $\Upsilon(1\text{S})$  and  $\Upsilon(2\text{S})$  samples, respectively, fix the parameters except for global normalization, then carry out the compound fit with 5 free parameters.

## 2.4 Determining the nuclear modification

The nuclear modification factor  $R_{\text{AA}}$  is a measure of modification of particle production in heavy ion collisions compared to what is naively expected from p+p collisions. It is defined as

$$R_{\text{AA}} = \frac{1}{\langle N_{\text{coll}} \rangle} \frac{\langle N_{\text{AA}} \rangle}{\langle N_{\text{pp}} \rangle}, \quad (3)$$

where  $\langle N_{\text{pp}} \rangle$  and  $\langle N_{\text{AA}} \rangle$  are the average numbers of produced particles in p+p and heavy ion collisions, and  $\langle N_{\text{coll}} \rangle$  is the average number of binary nucleon-nucleon collisions in a heavy ion collision.

Our generated samples correspond to  $10^7$   $\Upsilon$ -triggered 0-10% centrality Au+Au collisions and  $10^{10}$   $\Upsilon$ -triggered p+p events. The average number of binary collisions in 0-10% centrality range is  $\langle N_{\text{coll}} \rangle = 955 \pm 93$  [15].

## 2.5 Inferring the initial temperature

How much quarkonia of a given state melt in a heat bath depends on the initial temperature, the evolution of temperature over time, as well as the binding energy of the state. Since there is no way to calculate the correspondence between  $R_{\text{AA}}$  and the  $T_{\text{ini}}$  exactly, effective models are used. There are several concurrent models for that, using rather different approaches and assumptions, that naturally lead to a range of predictions [11, 12, 13]. There are, however, two limiting cases that are often used. In one, the heavy quark pair potential is based on the internal energy of the quark-antiquark system. This corresponds to a strongly bound scenario (SBS). In the other, the potential is based on the free energy, corresponding to a more weakly bound scenario (WBS). Models of Ref. [13] take into account both cold and hot nuclear effects on the quarkonium yield. Fig. 4 shows the  $R_{\text{AA}}(T_{\text{ini}})$  dependence results from these calculations both in the SBS and the WBS case. Note that we measure the total  $\Upsilon(1\text{S})$  yield. About half of the  $\Upsilon(1\text{S})$  mesons, however, come from cascade decays of excited Bottomonium states, eg.  $\chi_b$ ,  $\Upsilon(2\text{S})$ ,  $\Upsilon(3\text{S})$ . Even though the directly produced  $\Upsilon(1\text{S})$  yield is not strongly effected by the plasma, the melting of these higher states cause the total  $\Upsilon(1\text{S})$  yield to drop.

## 3 Summary of the tasks

The following steps of the measurement are expected to be completed.

1. **Determine the invariant mass distribution in the provided samples, corresponding to RHIC p+p and Au+Au collisions at  $\sqrt{s_{\text{NN}}} = 200$  GeV.** Use the mass window of 5-15 GeV/ $c^2$ .
2. **Optimize selection cuts for high-enough purity and efficiency.** Use simulated clean  $\Upsilon$  as well as background-only samples for this task.
3. **Determine the  $\Upsilon(1\text{S})$  and  $\Upsilon(2\text{S})$  yields.** To complete it, first determine the peak shapes by fitting the clean  $\Upsilon$  samples, then fit the p+p and Au+Au samples to separate signal from background.
4. **Compute the nuclear modification factor of  $\Upsilon(1\text{S})$  and  $\Upsilon(2\text{S})$  in RHIC Au+Au collisions at  $\sqrt{s_{\text{NN}}} = 200$  GeV, as well as the statistical errors. Explain the emerging pattern.**
5. **Infer the possible range of initial temperature of the strongly interaction Quark-Gluon Plasma at RHIC.** Use the SBS and WBS models of Ref. [13] as the two limiting scenarios. Are the models consistent with our observations?
6. *Bonus task: Observe the  $p_{\text{T}}$ -dependence of the nuclear modification. Eg. compare the  $R_{\text{AA}}$  for  $\Upsilon$  mesons with  $p_{\text{T}} < 3$  GeV/ $c$  and  $p_{\text{T}} > 3$  GeV/ $c$ . Do we understand what we see?*

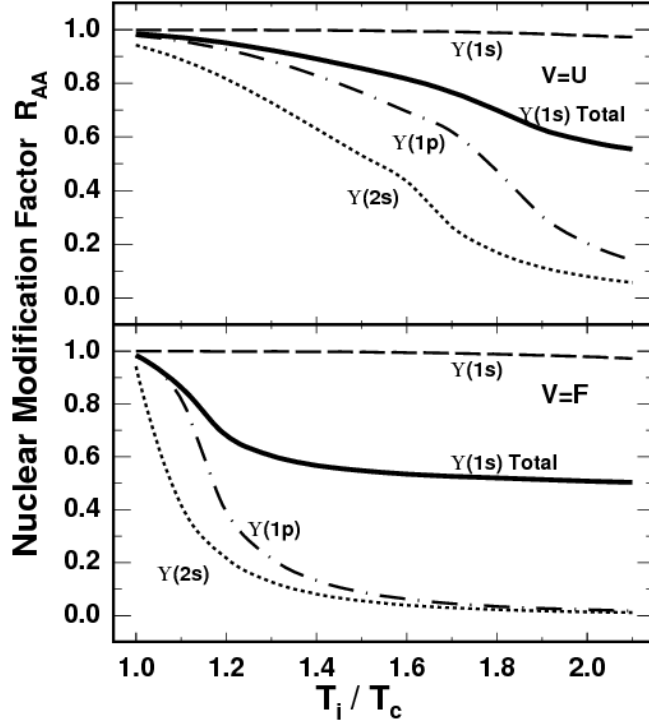


Figure 4: Initial temperature dependence of the nuclear modification factor  $R_{AA}$  in central Au+Au collisions. Taken from Ref. [13]. The strongly bound scenario is shown on the upper panel, the weakly bound scenario on the lower panel. The critical temperature of the deconfinement is  $T_c = 165$  MeV in this model ( $1 \text{ eV} = 11600 \text{ K}$ ).

## References

- [1] M. Csanád, “Alapvető mérések a nagyenergiás részecske- és magfizikában”, [http://atomfizika.elte.hu/haladolabor/docs/hep\\_leiras.pdf](http://atomfizika.elte.hu/haladolabor/docs/hep_leiras.pdf)
- [2] J. Adams *et al.* [STAR Collaboration], “Experimental and theoretical challenges in the search for the quark gluon plasma: The STAR Collaboration’s critical assessment of the evidence from RHIC collisions,” Nucl. Phys. A **757**, 102 (2005) [nucl-ex/0501009].
- [3] A. Adare *et al.* [PHENIX Collaboration], “Enhanced production of direct photons in Au+Au collisions at  $\sqrt{s_{NN}} = 200$  GeV and implications for the initial temperature,” Phys. Rev. Lett. **104**, 132301 (2010) [arXiv:0804.4168 [nucl-ex]].
- [4] T. Matsui and H. Satz, “ $J/\psi$  Suppression by Quark-Gluon Plasma Formation,” Phys. Lett. B **178**, 416 (1986).
- [5] Á. Mócsy and P. Petreczky, “Color screening melts quarkonium,” Phys. Rev. Lett. **99**, 211602 (2007). [arXiv:0706.2183 [hep-ph]].
- [6] M. I. Gorenstein, A. P. Kostyuk, H. Stöcker and W. Greiner, “Statistical coalescence model with exact charm conservation,” Phys. Lett. B **509**, 277 (2001) [hep-ph/0010148].
- [7] R. Rapp, D. Blaschke and P. Crochet, “Charmonium and bottomonium production in heavy-ion collisions,” Prog. Part. Nucl. Phys. **65**, 209 (2010) [arXiv:0807.2470 [hep-ph]].
- [8] V. Khachatryan *et al.* [CMS Collaboration], “Suppression of  $\Upsilon(1S)$ ,  $\Upsilon(2S)$  and  $\Upsilon(3S)$  production in PbPb collisions at  $\sqrt{s_{NN}} = 2.76$  TeV,” [arXiv:1611.01510 [nucl-ex]].

- [9] L. Adameczyk *et al.* [STAR Collaboration], “ $\Upsilon$  production in U + U collisions at  $\sqrt{s_{NN}} = 193$  GeV measured with the STAR experiment,” *Phys. Rev. C* **94**, no. 6, 064904 (2016) doi:10.1103/PhysRevC.94.064904 [arXiv:1608.06487 [nucl-ex]].
- [10] R. Vártesi, “Production of Quarkonia at RHIC,” *Int. J. Mod. Phys. A* **31**, no. 28n29, 1645036 (2016) doi:10.1142/S0217751X16450366 [arXiv:1510.00559 [nucl-ex]].
- [11] M. Strickland and D. Bazow, “Thermal Bottomonium Suppression at RHIC and LHC,” *Nucl. Phys. A* **879**, 25 (2012). [arXiv:1112.2761 [nucl-th]].
- [12] A. Emerick, X. Zhao and R. Rapp, “Bottomonia in the Quark-Gluon Plasma and their Production at RHIC and LHC,” *Eur. Phys. J. A* **48**, 72 (2012). [arXiv:1111.6537 [hep-ph]].
- [13] Y. Liu, B. Chen, N. Xu and P. Zhuang, “ $\Upsilon$  Production as a Probe for Early State Dynamics in High Energy Nuclear Collisions at RHIC,” *Phys. Lett. B* **697**, 32 (2011) doi:10.1016/j.physletb.2011.01.026 [arXiv:1009.2585 [nucl-th]].
- [14] [https://en.wikipedia.org/wiki/Crystal\\_Ball\\_function](https://en.wikipedia.org/wiki/Crystal_Ball_function) and references therein.
- [15] S. S. Adler *et al.* [PHENIX Collaboration], “Suppressed  $\pi^0$  production at large transverse momentum in central Au+Au collisions at  $\sqrt{s_{NN}} = 200$  GeV,” *Phys. Rev. Lett.* **91**, 072301 (2003) doi:10.1103/PhysRevLett.91.072301 [nucl-ex/0304022].